). Mexicana Astron. Astrof., 25, 39-50 (1993)

NEW GALACTIC ORBITS AND TIDAL RADII FOR GLOBULAR CLUSTERS

Christine Allen and Alfredo Santillán[1]

Instituto de Astronomía
Universidad Nacional Autónoma de México

Received 1992 October 13

RESUMEN

Se han calculado numéricamente las órbitas galácticas de seis cúmulos globulares empleando determinaciones recientes de sus movimientos propios absolutos en dos modelos para la distribución de masa galáctica; ambos modelos proporcionan una buena representación de la curva de rotación observada en la región comprendida entre 1 y 15 kpc, y una curva plana hasta 100 kpc. También se han recalculado las órbitas de tres cúmulos para los cuales se han obtenido recientemente valores mejorados de sus distancias y movimientos propios absolutos. Con las distancias pericéntricas resultantes de las órbitas integradas se han calculado los radios de marea esperados y se comparan éstos con los valores observacionales. Se evalúan los efectos de los errores de observación sobre los parámetros orbitales de los cúmulos, y sobre sus radios de marea. También se estudian las diferencias encontradas entre los resultados con los dos modelos para el potencial galáctico empleados.

ABSTRACT

The galactic orbits of six globular clusters have been numerically calculated in two different models for the galactic mass distribution, using recently determined absolute proper motions; both models give a good representation of the observed rotation curve in the region 1 to 15 kpc and a flat rotation curve out to 100 kpc. The orbits of three additional clusters with recent improved determinations of their distances and absolute proper motions have also been recalculated. With the pericentric distances resulting from the computed orbits, cluster tidal radii are determined, and these are compared with the observational values. The effects of observational errors upon the computed orbital parameters and tidal radii are evaluated. The differences found with both galactic models are also studied.

Key words: **CLUSTERS-DYNAMICS – GALAXY-STRUCTURE**

1. INTRODUCTION

Over the years, knowledge about the transverse ɔtions of globular clusters has been slowly accuılating. In a previous paper (Allen & Martos 88), we were able to collect absolute proper moı data for 10 globular and 3 galactic clusters; these systems, we computed the galactic orbits d tidal radii by direct numerical integration of ɛ equations of motion, using a galactic potential ɔdel previously developed by us. This study was ntinued when absolute proper motions for two ditional clusters became available (Allen 1990). General conclusions of both studies were that the observed tidal radii are a very poor indication of cluster perigalactica, and that they agree moderately well with the theoretical ones only if the perigalacticon corresponding to the last perigalactic passage is used. Further, it was found that there is practically no correlation of metallicity with orbital parameters, and that several orbits are, or verge on, being chaotic. The sensitivity of the orbital parameters to errors in the observed quantities was assessed, and it was found that the orbits are, in general, not greatly affected by such errors. The largest source of uncertainty was found to be the reduction from relative to absolute proper motion, and particularly, the size and direction assumed for the solar motion.

[1] Also at Dirección General de Servicios de Cómputo adémico, Universidad Nacional Autónoma de México.

In the intervening time, absolute proper motions for six additional clusters have become available. The results on M 4 (Cudworth & Rees 1990), M 28 (Rees & Cudworth 1991), and M 107 (Cudworth, Smetanka, & Majewski 1992) are part of an ongoing program that has produced by traditional methods the majority of presently available absolute proper motions for globular clusters. A novel method has been used recently for the clusters NGC 362 and 47 Tuc (Tucholke 1989, 1992*a*,*b*) both of which appear projected onto the Small Magellanic Cloud, thus allowing a direct determination of a quasi-absolute proper motion (i.e., relative to extragalactic stars) which can then be converted to absolute by allowing for the proper motion of the Magellanic Clouds themselves. In the case of NGC 6218 (M12), Brosche et al. (1991) have succeeded in determining the absolute proper motion with respect to distant galaxies, as they did earlier for NGC 5466 and NGC 4147.

In the present paper, the galactic orbits and tidal radii for the six new clusters are computed using the improved galactic potential model recently developed by us (Allen & Santillán 1991). The orbits of NGC 5466 and NGC 4147 are also recomputed in the newer potential model using improved values of their distances as was done by Brosche et al. (1991), and our results are compared with those obtained by them. A new orbit for M 92 is also obtained, using improved values for both the proper motion and the distance of this cluster, as given by Rees (1992). We also compute the orbits of all the clusters in the older potential model of Allen & Martos 1986 (hereinafter AM86), in order to assess the model dependency of the main results; furthermore, by computing two additional orbits for each cluster we attempt to take into account the dependency of the orbital characteristics upon the observational uncertainties, and we briefly discuss these results.

2. THE GALACTIC ORBITS

For the numerical integration of the orbits we will use a galactic mass model recently developed by Allen & Santillán (1991), which improves in several ways upon the earlier model that was used for previous studies. Although the new model is quite simple, it represents well the observed data most directly related to the quantities that shape a galactic orbit. The model consists of three components: a central spherical mass distribution and a disk, both of the Miyamoto-Nagai form, and a massive spherical halo. The resulting rotation curve is nearly flat from about 20 kpc out to 100 kpc, and agrees well with the observed values in the range 1 to 20 kpc. The run with z of the perpendicular force, K_z, computed from the model also agrees with observational data. The new values for the galactic constants advocated by the IAU have been taken, namely R_o = 8.5 kpc and V_o = 220 km s^{-1}; for the total local mass density ρ = 0.15 M$_\odot$ pc^{-3} was taken. The values for the rotation constants calculated from our mass model are A = 12.95 km s^{-1} kpc^{-1} and B = −12.93 km s^{-1} kpc^{-1}, in good agreement with recent determinations. With a cutoff for the halo at 100 kpc the total mass of the model galaxy is 9 × 10^{10} M$_\odot$. The new model potential is fully analytical, continuous, and with continuous derivatives; the density can be obtained from it in closed form, and is positive everywhere; the model is mathematically very simple, and allows rapid, accurate, and reproducible numerical orbit integrations.

Table 1 collects the observational data for the clusters under study. The values shown are those adopted by the authors of the absolute proper motion determination, except in the case of the distance to NCG 362, which was taken from Bolte's (1987) best fitting case. In the cases of both NGC 362 and 47 Tuc two sets of values for the proper motions are given. The first set corresponds to the absolute proper motion as determined with respect to stars of the SMC. The second set of values includes a correction for the proper motion of the SMC itself, assuming that it is equal to that of the LMC, which has been recently determined to be $\mu_\alpha \cos\delta$ = +0.9 mas y^{-1} and μ_δ = −0.2 mas y^{-1} (Tucholke & Hiesgen 1991). These two sets of values correspond to Tucholke's Cases 1 and 2. Table 2 lists the calculated galactocentric positions and velocities, which serve as "initial conditions" for the numerical integration of the orbits. The standard solar motion of 19.5 km s^{-1} in direction l = 56°, b = +23° was assumed (Delhaye 1965). For both M 4 and M 28 we repeated the reduction of relative to absolute proper motion in the standard manner, but using the galactic constants appropriate to our mass model instead of the ones adopted by Cudworth & Rees (1990) and Rees & Cudworth (1991); for M 107 Cudworth et al. (1992) apparently adopted the newer galactic constants, R_o = 8.5 kpc and V_o = 220 km s^{-1}, so no new reduction was necessary. The same holds true for the motion of M 92 (Rees 1992).

As in our previous work, we utilize a 7th order Runge-Kutta-Fehlberg algorithm with automatic step size control (Fehlberg 1968) for the numerical integration of the cluster orbits. The errors in the total energy and in the z-component of the angular momentum accumulated at the end of the orbit computations are generally of the order of $\Delta E/E = 10^{-6}$ and $\Delta h/h = 10^{-7}$. The orbits

TABLE 1

OBSERVED DATA FOR GLOBULAR CLUSTERS

Cluster	α (1950)	δ (1950)	d (kpc)	$\mu_\alpha \cos\delta$ (mas y^{-1})	μ_δ (mas y^{-1})	v_r (km s^{-1})
47 Tuc[1] (NGC 104)	$00^h\ 21.9^m$	$-72°\ 21.6'$	4.7	5.5	−1.6	−18.8
47 Tuc[2] (NGC 104)	00 21.9	−72 21.6	4.7	6.4	−1.8	−18.8
NGC 362[1]	01 01.5	−71 07.1	8.6	3.5	−2.6	217.0
NGC 362[2]	01 01.5	−71 07.1	8.6	4.4	2.8	217.0
NGC 4147	12 07.6	+18 49.2	16.1	−2.7	0.9	181.4
NGC 5466	14 03.2	+28 46.1	15.5	−5.4	0.6	107.2
M 4 (NGC 6121)	16 20.5	−26 24.4	2.0	−11.6	−16.3	71.0
M 107 (NGC 6171)	16 29.7	−12 56.7	6.2	−0.7	−3.1	−35.0
M 12 (NGC 6218)	16 44.6	−01 51.6	5.1	1.6	−8.0	−41.3
M 92 (NGC 6341)	17 15.6	+43 11.4	8.2	−4.6	−0.6	−120.5
M 28 (NGC 6626)	18 21.5	−24 53.8	5.1	0.4	−2.8	+15.9

TABLE 2

INITIAL CONDITIONS FOR GLOBULAR CLUSTERS

Cluster	ϖ (kpc)	z (kpc)	Π (km s^{-1})	Z (km s^{-1})	Θ (km s^{-1})
47 Tuc[1]	7.08	−3.32	24.53	33.07	185.01
47 Tuc[2]	7.08	−3.32	44.21	34.09	179.23
NGC 362[1]	7.40	−6.21	11.31	−69.03	−37.22
NGC 362[2]	7.40	−6.21	48.16	−61.62	−37.47
NGC 4147	10.14	15.70	148.57	162.26	222.23
NGC 5466	6.02	14.87	261.87	222.50	−106.93
M 4	6.61	0.55	−55.96	4.54	34.74
M 107	2.82	2.42	19.54	−42.23	148.03
NGC 6218	4.28	2.27	−38.48	−131.94	119.06
M 92	8.68	4.69	40.11	82.35	7.18
M 28	3.54	−0.50	6.52	−33.70	183.78

were computed backwards in time for an interval long enough to establish the character of the orbit, usually about 1.6×10^{10} years, a representative age for halo objects.

Table 3 lists the orbital parameters obtained from the integration of the cluster orbits. The columns are largely self explanatory. The last column contains the "eccentricity", calculated as $e = (R_{max} - R_{min})/(R_{max} + R_{min})$, where $R^2 = \varpi^2 + z^2$. Figures 1 to 10 show the orbits of some interesting clusters as projected on the meridional plane, as well as their surfaces of section. For each object two additional orbits were integrated, with the purpose of assesing the influence of observational errors on the computed orbital parameters. Table 4 lists the orbital parameters obtained from this experiment. We proceed to describe the salient features of each orbit as calculated in the newer potential. For the qualitative classification of the orbits we shall adhere to the scheme first developed by Ollongren (1962) and Torgard & Ollongren (1960) for axisymmetric, galactic-type potentials. A succinct and elementary description of this scheme can be found in Mihalas and Routly (1968). In the next section, these results will be compared with those obtained using the older potential, in order to assess their model dependency.

The orbit of 47 Tuc is a box of low eccentricity; in contrast to the case of M 28, which will be discussed below, the small eccentricity of 47 Tuc is hardly surprising since the cluster belongs to the high metallicity group of globular clusters, which is characterized by values of [Fe/H] > −0.8. Its metallicity is given as [Fe/H] = −0.71 (Armandroff & Zinn 1988). The box remains radially confined in the region between 5.6 and 8.0 kpc, and attains z values of 3.76 kpc. As can be seen in Table 3 the orbit does not change appreciably if instead of the absolute proper motion (Case 2) we use the value without the correction for the motion of the LMC

TABLE 3

PARAMETERS OF GALACTIC ORBITS OF GLOBULAR CLUSTERS

Cluster	E	h	w_{min}	w_{max}	z_{min}	z_{max}	e
	(100 km^2 s^{-2})	(10 km kpc s^{-1})	(kpc)		(kpc)		
47 Tuc[1]	−1241.46	131.01	6.1	7.7	−3.6	3.6	0.117
47 Tuc[2]	−1244.87	126.93	5.6	8.1	−3.8	3.8	0.177
NGC 362[1]	−1280.00	−27.53	0.8	10.4	−8.3	8.2	0.853
NGC 362[2]	−1273.78	−27.73	0.5	11.7	−6.2	6.4	0.915
NGC 4147	−546.89	225.35	6.1	61.9	−52.1	51.4	0.819
NGC 5466	−445.46	−64.36	1.5	82.8	−81.0	81.8	0.965
M 4	−1522.39	22.96	0.5	6.9	−4.0	1.7	0.879
M 107	−1590.31	41.80	2.1	3.5	−2.5	2.5	0.253
NGC 6218	−1457.70	50.98	2.1	5.7	−3.7	3.7	0.474
M 92	−1273.54	6.23	0.1	11.3	−8.7	7.7	0.978
M 28	−1637.14	65.04	3.0	3.6	−0.6	0.6	0.082

TABLE 4

PARAMETERS OF GALACTIC ORBITS OF GLOBULAR CLUSTERS WITH OBSERVATIONAL UNCERTAINTIES

Cluster	E	h	w_{min}	w_{max}	z_{min}	z_{max}	e
	(100 km^2 s^{-2})	(10 km kpc s^{-1})	(kpc)		(kpc)		
47 Tuc[1]+	−1113.77	166.01	6.8	11.6	−5.5	5.5	0.264
47 Tuc[1]−	−1329.14	96.02	3.7	7.7	−3.3	3.3	0.354
47 Tuc[2]+	−1114.82	161.98	6.5	11.7	−5.7	5.7	0.286
47 Tuc[2]−	−1334.80	91.87	3.5	7.8	−3.4	3.4	0.387
NGC 362[1]+	−1299.73	2.60	< 0.1	11.2	−7.1	5.8	0.993
NGC 362[1]−	−1238.11	−57.67	2.1	10.3	−7.9	7.9	0.674
NGC 362[2]+	−1290.56	2.55	< 0.1	11.3	−8.2	8.2	0.993
NGC 362[2]−	−1234.68	−58.00	1.9	10.8	−7.4	7.4	0.702
NGC 4147+	−38.07	352.56	8.6	591.4	−819.4	15.5	0.971
NGC 4147−	−854.05	98.14	2.7	28.0	−23.7	23.6	0.822
NGC 5466+			escapes				
NGC 5466−	−721.03	−86.04	2.3	39.9	−37.0	37.1	0.890
M 4+	−1513.90	36.40	0.9	6.8	−3.2	3.3	0.780
M 4−	−1526.02	9.85	0.2	6.9	−4.8	4.5	0.951
M 107+	−1546.42	50.02	2.6	3.7	−2.6	2.6	0.167
M 107−	−1616.68	33.57	1.5	3.9	−2.7	2.7	0.453
NGC 6218+	−1465.77	62.16	2.8	5.1	−3.1	3.1	0.290
NGC 6218−	−1425.95	39.81	1.5	6.7	−4.7	4.6	0.643
M 92+	−1178.64	27.69	0.6	13.7	−9.0	8.9	0.912
M 92−	−1299.42	−15.23	0.3	10.3	−7.7	7.7	0.944
M 28+	−1602.14	72.03	3.4	3.8	−0.5	0.5	0.050
M 28−	−1665.48	58.04	2.5	3.6	−0.7	0.7	0.171

(Case 1). The values for the maximum R and z attained by this cluster do not vary significantly either. Adding and subtracting observational uncertainties has the effect of radially shifting and elongating this orbit (see Table 4), but does not change its qualitative character.

The cluster NGC 362 represents an example of a highly eccentric orbit, which visits the innermost region of the Galaxy. When we use the absolute proper motion (Case 2) the orbit is clearly chaotic. The meridional orbit is shown in Figure 1, the surface of section in Figure 2. The radial excursions span the range between R = 0.53 kpc and R = 11.7 kpc; the vertical motion is confined to the region between z = −6.2 kpc and z = +6.4 kpc. Due to the chaotic nature of the orbit, however, these extrema may be different if the orbit is computed for a longer time, since energy conversion from planar into vertical motion and viceversa takes place continuosly. When the orbit is computed using the proper motion relative to the SMC (Case 1) it is still chaotic, but already shows some similarity to a box. The perigalactic distance reached by this orbit is just over 1 kpc, and thus almost a factor of 2 larger than in Case 2, a fact which perhaps accounts for the the orbit verging on chaotic, but already resembling a box. Other orbital parameters are seen to remain quite similar in both Cases 1 and 2. The metallicity of this cluster is listed as [Fe/H] = −1.28 (Armandroff & Zinn 1988), and would be compatible with a less extreme orbit.

The orbit for NGC 4147 was recalculated using the improved observational data given by Brosche et al. (1991) in both our galactic models. Contrary to the statement of Brosche et al. that the orbit is a tube in the older potential model, we find the orbit to be of box type. Brosche et al.'s Figure 1b , showing the meridional orbit of this cluster is in fact nearly identical to Figure 5 in our previous paper (Allen & Martos 1988), but

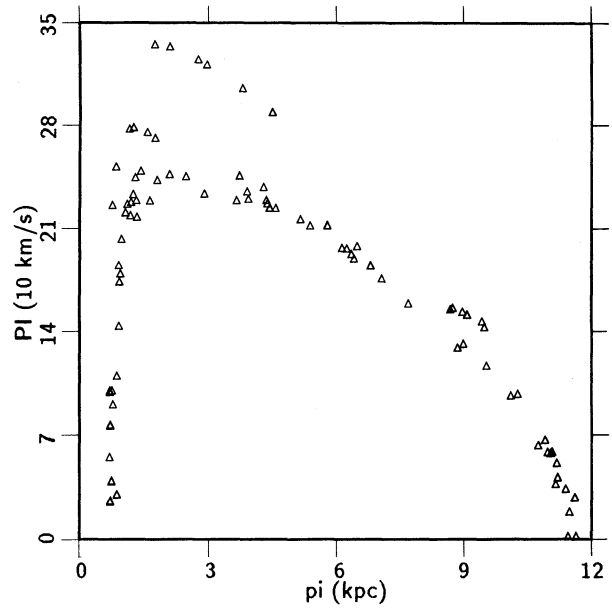

Fig. 2. The surface of section of NGC 362, Case 2.

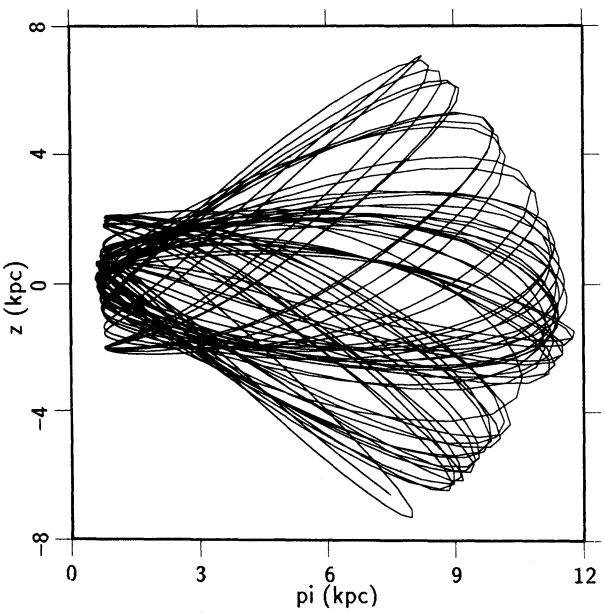

Fig. 1. The meridional orbit of NGC 362, Case 2.

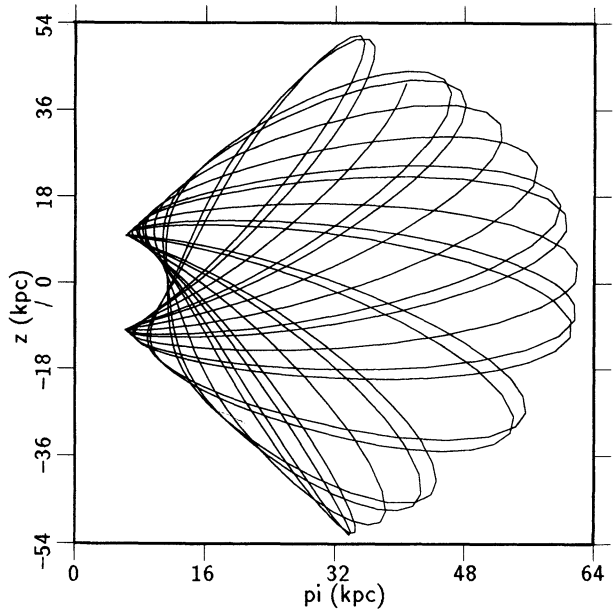

Fig. 3. The meridional orbit of NGC 4147.

we classified the orbit as a box. Figures 3 to 6, showing the meridional orbits and the surfaces of section for this cluster demonstrate that the orbit is, in fact, a box in both the older and the newer potential models, and that it shows no north-south asymmetry. The discrepancy between our results and those of Brosche et al. can be attributed solely to the fact that these authors computed the orbit for a shorter span of time, of the order of 10^{10} years, not sufficiently long to allow a reliable characterization. After 1.6×10^{10} years the symmetric box character of the orbit is clearly seen. This cluster reaches very large galactocentric distances of over 62 kpc. Its z-values are also extremely high, attaining over 53 kpc. The orbit has an eccentricity of 0.82. A comparison of the orbital parameters with those given by Brosche et al. shows some quantitative differences; they are, however, not very significant. The metallicity of this cluster, [Fe/H] = −1.80 (Zinn 1985), places it clearly among the group of metal poor clusters, in good concordance with the character of its orbit.

The orbit of the cluster NGC 5466, which was also recalculated using newer parameters (Brosche et al. 1991) turns out to be quite similar to the one we had found in the older potential with slightly different observational parameters. In particular, the new cluster distance is somewhat larger. Like in the case of NGC 4147, the orbit is of box type, and reaches extremely large galactocentric distances, R_{max} = 84.4 kpc. The metallicity of this cluster, [Fe/H] = −2.22 (Zinn 1985) makes it one of the metal-poorest in our sample, a fact which is quite compatible with its orbit. Although the general character of the orbit is similar to that obtained by Brosche et al. (1991), there are quantitative differences in the orbital parameters. These differences, however, are well within the uncertainties arising from observational errors.

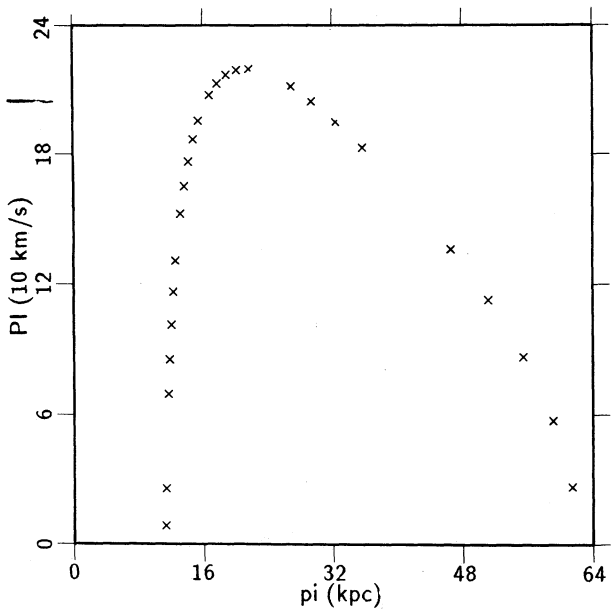

Fig. 4. The surface of section of NGC 4147.

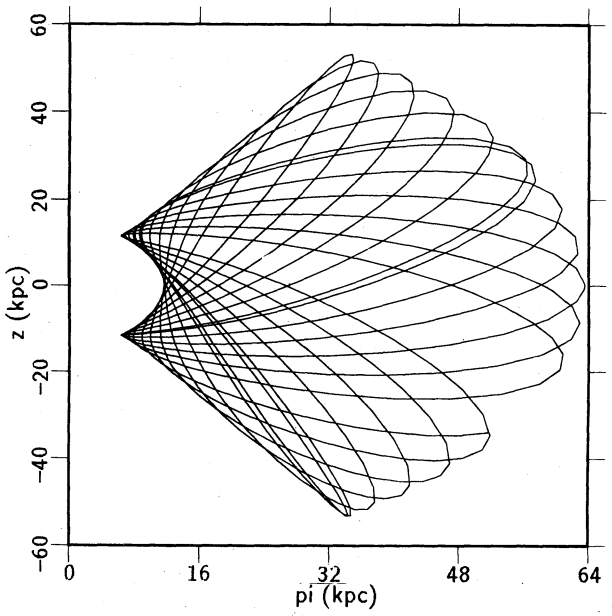

Fig. 5. The meridional orbit of NGC 4147, computed with the AM86 potential.

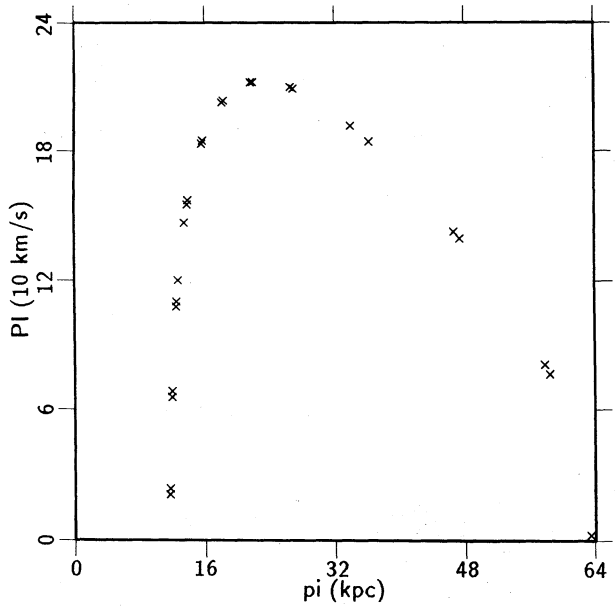

Fig. 6. The surface of section of NGC 4147, computed with the AM86 potential.

The orbit of M 4 is quite eccentric (e = 0.879), ınd takes this cluster close to the galactic center R_{min} = 0.446 kpc). Both the meridional diagram ınd the surface of section (Figures 7 and 8) how this orbit to be chaotic, and while the z_{max} eached by this cluster is about 1.5 kpc during ong periods of time, at other times it reaches ılmost 4 kpc; were we to compute the orbit over ı longer time even larger values of z_{max} are ıot excluded, since the chaotic character of the ›rbit allows efficient conversion of planar into z-notion. Contrary to the assertion of Cudworth & Rees (1990), we find that the orbit of M 4 is ıot confined to the disk, and its current height ıbove the plane, z = 0.55 kpc, is much smaller han the maximum height the cluster reaches in he course of its galactic orbit; (the reason for his discrepancy is that Cudworth & Rees, not ıaving integrated the full orbit, were unaware of ts chaotic nature; they estimated the maximum ;-value from the current Z-velocity of the cluster, ınd did not take into account the conversion of ›lanar into vertical motion characteristic of chaotic ›rbits). Furthermore, we find that in the context ›f the large eccentricity of its galactic orbit, and of he fact that its z_{max} reaches values of about 4 kpc, he moderately low value for the metallicity of M 4, [Fe/H] = −1.28 (Zinn 1985), is not surprising. The haotic nature of the orbit of M 4 persists when it is computed taking into account the observational ıncertainties; both computed orbits are chaotic. Table 4 shows the resulting changes in the orbital parameters.

M 107 is a cluster whose orbit exhibits very small radial oscillations –the orbit is a box confined between 2.0 and 3.5 kpc; in contrast, its z-oscillations reach more than 5 kpc in total, ranging from −2.5 to +2.5 kpc. Its metallicity, listed as [Fe/H] = −0.99 (Zinn 1985) could be an indication that M 107 belongs to the thick disk. The large values of z attained by this cluster, however, point to M 107 belonging to the halo population.

The orbit of M 12 is also a box, similar to that of M 107 in that its radial oscillation (from 2 to 5.8 kpc) is smaller than its z-oscillation (from −3.8 to +3.8 kpc). It is quite similar to that obtained by Brosche et al. using our older potential model. The metallicity of this cluster, [Fe/H] = −1.61 (Zinn 1985), places it among the metal poor group of clusters; the form of its orbit and the z-values attained point to a typical population II object.

The orbit of M 92 represents another interesting example of an object visiting the innermost regions of the Galaxy. This cluster attains an R_{min} of 0.73 kpc, and its orbit has an eccentricity of 0.97, the largest among the clusters computed. The radial oscillation takes the cluster out to distances of about 12 kpc. Its orbit is clearly chaotic, as shown in Figures 9 and 10. The cluster spends about half of the computed time in a relatively flat orbit, resembling an asymmetric tube and reaching z-values of less than about 1 kpc, but then energy conversion from planar into z-motion takes place, and during the latter half of its evolution, the orbit reaches a maximum z of over 8 kpc. This orbit is illustrative of the

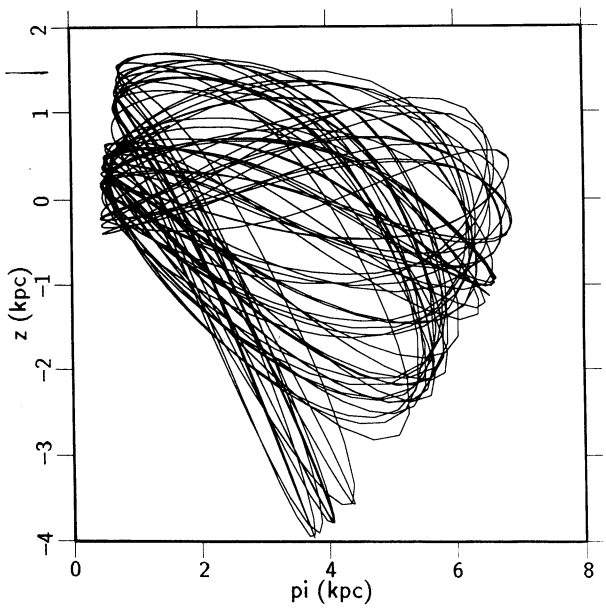

Fig. 7. The meridional orbit of M 4.

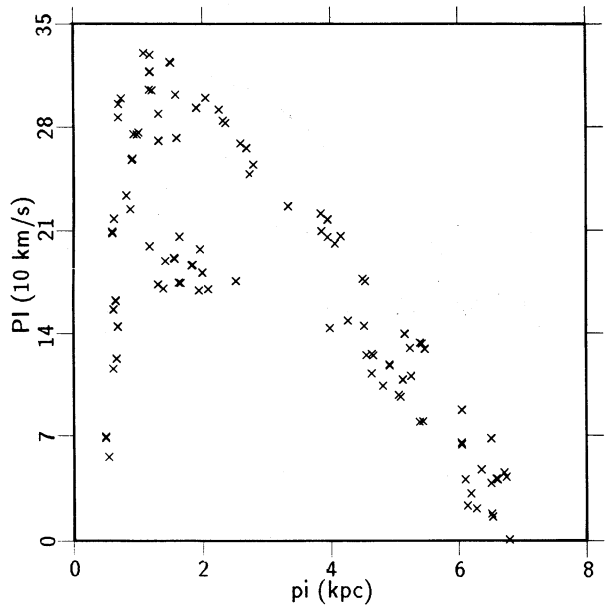

Fig. 8. The surface of section of M 4.

fact that present positions and motions of globular clusters may not have anything to do with the values they had at other times of their lives, and that even when their full space motions are known, they have to be interpreted with caution. The metal content of this cluster, [Fe/H] = −2.24 (Zinn 1985), marks this cluster as the metal-poorest of our sample, in good agreement with the extreme character of its orbit.

The cluster M 28 turns out to have a remarkable orbit. It is confined radially between 3.0 and 3.6 kpc. The orbit is a symmetric box, and its eccentricity is the smallest of all the cluster orbits we have calculated (e = 0.08); it is even smaller than that of the galactic clusters NGC 188 and M 67 (e = 0.11 for both) and NGC 2420 (e = 0.32) (Allen & Martos 1988); during its z-oscillation the cluster reaches a height of only 0.576 kpc. Thus, we concur with Rees & Cudworth (1991) in finding the orbit of this cluster surprising for an object of fairly low metallicity. However, the metallicity of this cluster has been the subject of a lively controversy. Values as low as [Fe/H] = −1.81 and as high as [Fe/H] = −1.0 have been given in the recent literature (see Rees & Cudworth 1991 for a discussion of this problem). Indeed, the orbital parameters are most characteristic of a thick disk object, and would seem to be consistent with the higher values of the metallicity. Although the metallicity of thick disk objects may in fact be as low as [Fe/H] = −1.6, this is really a rather extreme value for such objects. The only other globular clusters with comparable orbital characteristics are M 71, with an eccentricity of 0.21 (Allen & Martos 1988), and 47 Tuc (e = 0.18), whose orbit is here presented and was discussed earlier. Both these clusters have, however, relatively high metallicities, [Fe/H] = −0.58 and −0.71, respectively, as tabulated by Zinn (1985), and Armandroff & Zinn (1988), and thus they definitely belong to the high-metallicity group of globular clusters, whereas M 28 –even assuming the highest metallicity value– clearly does not belong to this group. As can be seen in Table 4, the orbital characteristics of M 28 do not change appreciably when observational uncertainties are taken into account. In particular, the incompatibility between the low values for the metallicity and the disk-type orbit remains.

The orbital parameters computed taking into account observational errors are collected in Table 4. As previously mentioned, two additional orbits were computed for each object, obtained by adding to, and subtracting from, the space velocities the uncertainties resulting from observational errors as indicated by Johnson & Soderblom (1987). These orbits are designated as "+" and "−" respectively. Table 4 shows the variations in the orbital parameters that are to be expected as a consequence of observational uncertainties. The largest discrepancies are found for the clusters most weakly bound to the Galaxy, namely NGC 4147 and NGC 5466. In fact, the orbit obtained for NGC 5466+ has positive energy, and is thus an escape orbit. The orbit of NGC 4147+ is only marginally bound to the Galaxy, and so its parameters are very uncertain. Since both clusters

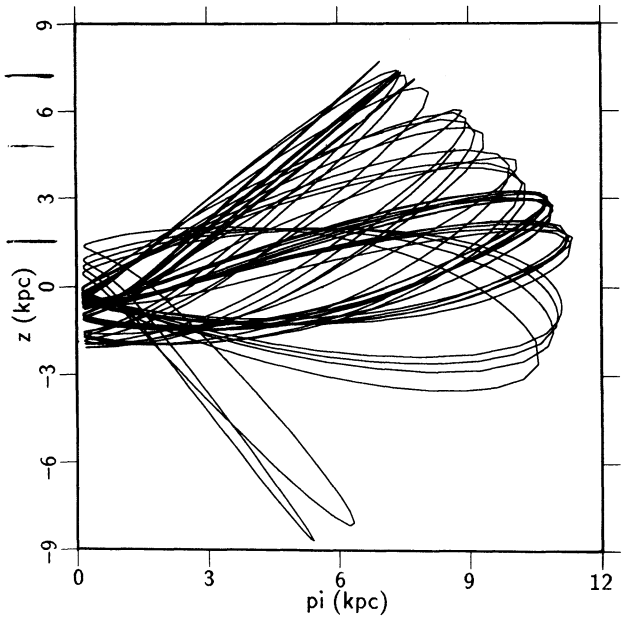

Fig. 9. The meridional orbit of M 92.

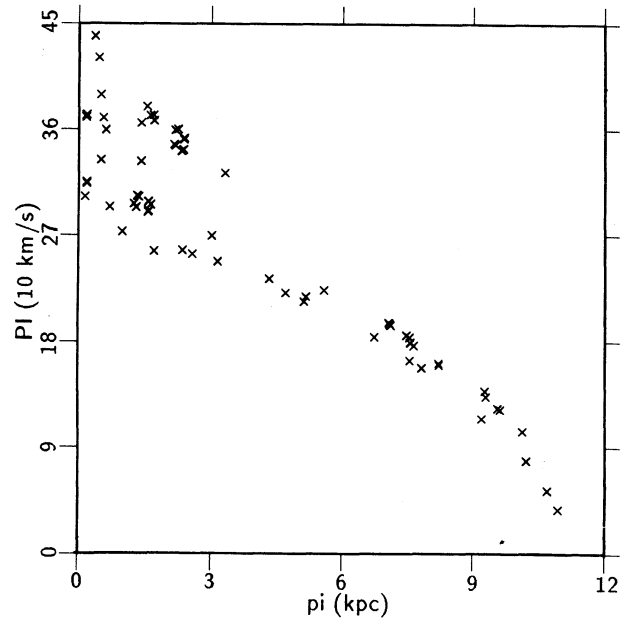

Fig. 10. The surface of section of M 92.

TABLE 5

PARAMETERS OF GALACTIC ORBITS OF GLOBULAR CLUSTERS
(AM86 POTENTIAL)

Cluster	E	h	w_{min}	w_{max}	z_{min}	z_{max}	e
	(100 km^2 s^{-2})	(10 km kpc s^{-1})	(kpc)		(kpc)		
47 Tuc[1]	−1243.86	134.22	7.0	8.1	−3.7	3.8	0.108
47 Tuc[2]	−1236.74	130.63	5.9	8.0	−3.7	3.7	0.151
NGC 362[1]	−1307.79	−23.35	0.5	11.1	−7.2	6.8	0.912
NGC 362[2]	−1302.84	−22.27	0.5	10.8	−7.3	7.1	0.908
NGC 4147	−586.14	221.91	6.3	63.5	−53.3	53.2	0.819
NGC 5466	−483.74	−63.72	1.6	84.3	−81.9	81.6	0.963
M 4	−1585.31	24.14	0.5	6.4	−0.6	0.9	0.855
M 107	−1586.90	35.48	2.2	2.9	−2.5	2.5	0.122
NGC 6218	−1475.14	47.63	2.2	5.5	−3.5	3.5	0.426
M 92	−1304.08	7.29	0.2	10.8	−2.1	6.3	0.969
M 28	−1720.98	57.44	2.7	3.1	−0.5	0.5	0.785

are undoubtedly members of our Galaxy, this result indicates that at least in the (+) direction the observational errors cannot be as large as quoted. It is also worth remarking that these two clusters would not be bound at all to a galaxy even slightly less massive than the model we have used. In two other cases, namely M 4 and M 92, the qualitative character of the orbit changes, although other orbital parameters remain comparable. We note also that orbits with small angular momentum, like those of NGC 362 and M 4, show the largest variations in perigalactic distance. Furthermore, NGC 362 and M 92 –both having very small angular momenta– are seen to reverse their sense of rotation about the Galaxy in the two additional orbits computed. In all other cases it can be seen that in general, the orbital parameters do not vary significantly. We can therefore conclude that the orbital parameters are not very sensitive to the precise values taken as initial conditions, at least when they vary within the range of the errors quoted by observers.

3. COMPARISON WITH THE OLDER POTENTIAL MODEL

Table 5 shows the orbital parameters obtained with the AM86 potential model. In general, no major differences are seen, especially if one considers that both models incorporate different galactic constants. Table 6 presents a summary of the orbital classification for all computed cases. A box orbit is denoted by *b*, a tube orbit by *t*, a shell orbit by *s*, and chaotic orbits by *c*; borderline cases

TABLE 6

CLASSIFICATION OF GALACTIC ORBITS
OF GLOBULAR CLUSTERS

	New Potential			AM86 Potential
Cluster	Orbit (0)	Orbit (+)	Orbit (−)	Orbit (0)
47 Tuc[1]	b	b	b	b
47 Tuc[2]	b	b	b	b
NGC 362[1]	c	c	s	c
NGC 362[2]	c	c	b	c
NGC 4147	b	b	b	b
NGC 5466	b	...	b	b
M 4	c	c	c	bc
M 107	b	b	b	b
NGC 6218	b	b	b	b
M 92	c	bc	bc	tc
M 28	b	b	b	b

are indicated by a combination of letters. Based on the comparison of Tables 3 and 5, we can conclude that orbital parameters such as the maximum *z*-distance or the peri- or apogalactic distance do not depend sensitively on the particulars of the adopted galactic mass model. A large fraction of the differences shown in the orbital parameters of Table 5 can, in fact, be attributed solely to the difference in R_o and $V(R_o)$ in both galactic models. However, two of the orbits do show a qualitati-

vely different behaviour in both potentials. One is the orbit of M 4 which verges on chaotic in the AM86 model, whereas it is clearly chaotic in the newer model. The other is that of M 92, a tube with some evidence of chaos in the AM86 potential, and a definitely chaotic orbit in the newer potential. Still, it is surprising that the qualitative differences displayed by the orbits of these two clusters are relatively minor. Note that these two clusters also exhibited particularly large differences in some of their parameters when computed with observational errors, as shown in Table 4. Clearly, their orbits are located in peculiar regions of phase space.

4. THE TIDAL RADII

Table 7 displays the theoretical tidal radii and compares them with the observed values, calculated from Webbink's (1985) data and the distances of Table 1. Consecutive columns contain the observed limiting radii and the theoretical tidal radii computed by means of King's (1962) formula, using the perigalactic distances for the times of last passage through perigalacticon, as well as the minimum perigalactic distance ever reached by the cluster in the course of its computed galactic orbit; for M_G , the "effective" galactic mass, we used the equivalent point mass that produces the true force acting on the cluster at the perigalactic point, as computed from the galactic mass model. To estimate cluster masses from their integrated visual luminosities an M/L ratio of 1.6 was assumed throughout (Illingworth 1976). The subscripts d and r refer to direct and retrograde orbits of star within the cluster, and their relevance will be discussed below.

As can be seen from Table 7 the agreemen between theoretical and observed values is not i every case satisfactory. The largest discrepancie are found for the clusters M 4 and M 107, whos observed limiting radii are much larger than th theoretical ones, and M 28, which shows a discre pancy in the opposite sense. Note that the lar ger distance assumed in the present paper fo NGC 5466 implies a larger observed limiting radi us, somewhat larger than the theoretical one. Wit the distance used previously, a closer agreemen between theoretical and observed limiting radiu was found (Allen & Martos 1988).

In order to test whether the the discrepancie found could be ascribed to observational uncer tainties in the cluster parameters, we calculate the tidal radii corresponding to the two addition al orbits obtained for the most discrepant cluster namely NGC 5466, M 4, M 107 and M 28. Table shows, however, that except in the cases of patho logical orbits, like those of NGC 362 and M 4, th differences found for ϖ_{min} and z_{min} are not large so that no great variations in the calculated tid al radii are to be expected. This is in fact s Table 8 shows the result of this test. It is read ily seen that the large discrepancies in the cas of M 4 are not resolved; for M 107 and M 28 th agreement improves somewhat. For NGC 546 the distance given by Brosche et al. (1991) ma be an overestimate, since a more moderate valu

TABLE 7

OBSERVED AND COMPUTED LIMITING RADII FOR GLOBULAR CLUSTERS

Cluster	m_c	r_t(observed)	r_t(last)	r_t(min)	$r_t(\text{last})_d$	$r_t(\text{last})_r$
	(10^5 $M_\odot$)	(pc)	(pc)			
47 Tuc[1]	9.38	61.1	104.8	106.2	72.6	145.2
47 Tuc[2]	9.38	61.1	100.5	100.8	69.7	132.3
NGC 362[1]	2.94	25.6	35.5	18.3	24.6	49.2
NGC 362[2]	2.94	25.6	29.2	11.4	20.2	40.4
NGC 4147	0.34	33.9	48.4	46.7	33.5	67.1
NGC 5466	0.87	94.2	47.2	44.7	32.7	65.4
M 4	0.82	25.4	7.1	7.1	4.9	9.8
M 107	0.78	41.3	24.8	24.7	17.2	34.4
NGC 6218	1.36	27.0	30.0	28.1	20.8	41.6
M 92	2.31	39.6	28.3	1.3	19.6	39.2
M 28	2.44	22.5	42.7	42.8	29.6	59.2

TABLE 8

OBSERVED AND COMPUTED LIMITING RADII FOR GLOBULAR CLUSTERS WITH OBSERVATIONAL UNCERTAINTIES

Cluster	m_c	r_t(observed)	r_t(last)	$r_t(\text{last})_d$	$r_t(\text{last})_r$
	(10^5 $M_\odot$)	(pc)	(pc)	(pc)	
NGC 5466+	0.87	90.2	escapes	...	...
NGC 5466−	0.87	90.2	43.1	28.9	59.8
M 4+	0.82	25.4	10.8	7.5	15.0
M 4−	0.82	25.4	5.0	3.4	6.9
M 107+	0.78	41.3	28.3	19.6	39.2
M 107−	0.78	41.3	19.2	13.8	27.6
M 28+	2.44	22.5	45.1	29.2	58.4
M 28−	2.44	22.5	37.1	25.7	51.5

ıds to agreement between computed and obser-
d limiting radius (Allen & Martos 1988), and
akes the orbit less prone to escape. Hence, we
nclude that in order to be responsible for the
screpancies found in the tidal radii, the observa-
ınal errors would have to be much larger than
e those quoted, at least for these clusters. But in
:t we pointed out earlier that in the cases of both
GC 4147 and NGC 5466 we may suspect that
e observational errors have been overestimated,
least in the "+" direction. Whether or not it is
alistic to assume larger errors, particularly in the
stances and proper motions, is a question that
ıly future observational work can settle.

One could suppose that the discrepancies found
uld be the result of uncertainties in the com-
ıted orbits stemming from the mass model used.
owever, previous work using Schmidt-type po-
ntials (Allen & Moreno 1981), as well as the re-
lts here presented, show that the computed or-
ts, and in particular, the perigalactic distances
e not very sensitive to the galactic potential used.
ıble 5 shows that the differences found amount
most to about 10% (after scaling to compensate
r different galactic parameters used). So, it can
: concluded that the discrepancies found are not
e result of particulars of the mass model used,
ıd thus unlikely to be resolved using other mass
odels.

On the theoretical side, the situation concerning
niting radii is far from satisfactory. As is now
:nerally well known, the classical King formula,
:hough widely used, does not yield a reliable es-
nate of the actual limiting radius of a cluster.
ıe tidal radius computed from King's formula
ıpears to be an overestimate, which should be
duced by a factor of 0.693 (Innanen, Harris, &
Webbink 1983) for direct orbits; retrograde orbits can be retained by the cluster for radii of up to twice this corrected limiting radius over very long times. This is the reason why we show in Tables 7 and 8 also the tidal radii for direct and retrograde orbits of cluster stars. If the tidal radius is set mainly at the times of perigalactic passage, then the observed limiting radii should be closer to the value corresponding to the last perigalactic passage than to those of previous passages (except, of course, in the rare cases where the cluster relaxation time greatly exceeds the orbital period around the galaxy, or where the cluster has just passed through perigalacticon). In any case, the tidal radii observed at any given time are influenced not only by the action upon the cluster of the galactic tidal field, but by many other dynamical effects, like tidal shocks when crossing the galactic plane, encounters with massive clouds or spiral arms, etc., as well as by the cluster's own relaxation and dynamical evolution. Therefore, in addition to the large observational uncertainties involved in the determination of limiting radii, the only simple theoretical estimate of the tidal radii, namely King's formula, appears to be of doubtful applicability. A re-examination of this problem, based on a more realistic modelling of the relevant dynamical effects is undoubtedly needed, but clearly beyond the scope of the present paper.

5. SUMMARY AND CONCLUSIONS

We have presented the galactic orbits of six globular clusters. The orbits were obtained by direct numerical integration of the equations of motion, assuming a realistic mass model for the Galaxy, and using the observed values for the radial

and transverse velocities of the clusters as well as their distances to compute "initial conditions" for the numerical integration. Orbital parameters resulting from the numerical integration are shown to be relatively insensitive to the particulars of the galactic mass model used, as well as to the observational errors likely to be present in cluster distances and motions. With the data provided by the computed orbits, we have used King's formula to estimate the theoretical tidal radii for these clusters, taking the perigalactic distances at the time of their last perigalactic passage. The agreement between theoretical and observed limiting radii is not always satisfactory. The differences found cannot be attributed to either observational errors or particulars of the mass model used, since orbital parameters are shown to be quite insensitive to such errors, and nearly model-independent. Whether or not the discrepancies might be resolved by a more sophisticated theoretical treatment of the tidal radii cannot at present be settled.

The authors are grateful to H.J. Tucholke for sharing his results on the motions of NGC 362 and 47 Tuc prior to publication.

REFERENCES

Allen, C. 1990, RevMexAA, 20, 137
Allen, C., & Martos. M.A. 1986, RevMexAA, 13, 137
_____. RevMexAA, 16, 25
Allen, C., & Moreno, E. 1981, unpublished
Allen, C., & Santillán, A. 1991, RevMexAA, 22, 255
Armandroff, T.E., & Zinn, R. 1988, AJ, 96, 92
Bolte, M. 1987, ApJ, 315, 469
Brosche, P., Tucholke, H.J., Klemola, A.R., Nincovic, S
Geffert, M., & Doerenkamp, P. 1991, AJ, 102, 2022
Cudworth, K.M., & Rees, R. 1990, AJ, 99, 1491
Cudworth, K.M., Smetanka, J.J., & Majewski, S.R. 199
AJ, 103, 1252
Delhaye, J. 1965, in Galactic Structure, eds. A. Blaau
& M. Schmidt (Chicago: The University of Chica
Press), 61
Fehlberg, E. 1968, NASA TR R-287
Illingworth, G. 1976, ApJ, 204, 73
Innanen, K.A., Harris, W., & Webbink, R.F. 1983, AJ, 8
338
Johnson, D.R.H., & Soderblom, D.R. 1987, AJ, 93, 864
King, I.R. 1962, AJ, 67, 471
Mihalas, D., & Routly, P.M. 1968, in Galactic Astronom
(San Francisco: Freeman), 226
Ollongren, A. 1962, BAN, 16, 241
Rees, R., & Cudworth, K.M. 1991, AJ, 102, 152
Rees, R. 1992, AJ, 103, 1573
Torgard, I.H.M., & Ollongren, A. 1960, NUFFIC Con
Netherlands
Tucholke, H.-J. 1989, Ph.D. Thesis, Westfälische Wilhelm
Universität, Münster
_____. 1992*a*, A&AS, 93, 293
_____. 1992*b*, A&AS, 93, 311
Tucholke, H.-J., & Hiesgen, M. 1991, in IAU Symposiu
148, The Magellanic Clouds, eds. R.F. Haynes & D.
Milne (Dordrecht: Kluwer), 491.
Webbink, R.F. 1985, in Dynamics of Star Clusters, eds.
Goodman & P. Hut (Dordrecht:Reidel), 541
Zinn, R. 1985, ApJ, 293, 424

Christine Allen and Alfredo Santillán: Instituto de Astronomía, UNAM, Apartado Postal 70-264, 0451 México, D.F., México.